Search for Roma-BZCAT Blazars in the Palermo BAT Survey archive

B. Sbarufatti[*][,a] **V. La Parola, G. Cusumano, V. Mangano, A. Segreto, P. Romano**

INAF-IASFPa
Via U. La Malfa 153
I-90146 Palermo
Italy
[a]*E-mail:* sbarufatti@ifc.inaf.it

S. Campana, G. Chincarini, G. Tagliaferri

INAF-OAB
via E. Bianchi 46
I-23807 Merate
Italy

P. Giommi

ASDC
via Galileo Galilei
I-00044 Frascati
Italy

Blazars are the most numerous class of extragalactic $\gamma-$ray sources. Because of their very broad spectral emission, blazars are expected to play an important role in the generation of the extragalactic background in several energy bands. Using the Palermo BAT survey archive we searched for the hard X-ray counterparts of the $\sim$2600 objects in the Roma-BZCAT Blazars catalogue to study their contribution to the 15–150 keV extragalactic emission.
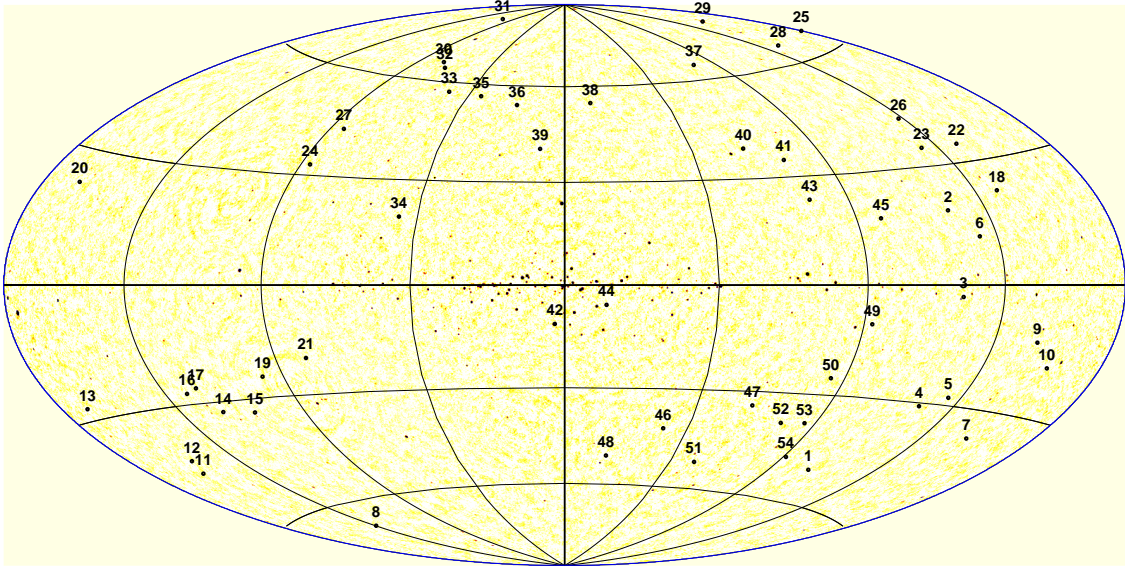
7th INTEGRAL Workshop
September 8-11 2008
*Copenhagen, Denmark*

---

[*]Speaker.

Figure 1: Palermo BAT Survey map of the sky in galactic coordinates. Blazars from the Roma-BZCAT catalogue detected above a 4.8 σ level in the Palermo BAT Survey are shown.

The BAT survey archive consists of data collected by the Burst Alert Telescope [1] on board of the Swift spacecraft [2] while the observatory waits for Gamma ray Bursts (GRBs). Our team is exploiting observations from the first 39 months of the Swift mission through a systematic search for new hard X-ray sources by means of the BatImager [4], a dedicated software, completely independent from the one developed by the Swift-BAT hardware team, to process the BAT survey data.

The Roma-BZCAT (http://www.asdc.asi.it/bzcat) is a catalogue of blazars based on multi-frequency surveys and an extensive review of the literature ([3]). It contains ∼2600 sources, classified either as BL Lac objects, Flat Spectrum Radio Quasars and blazars of uncertain/unknown nature. We searched for the counterparts of these sources in the BAT survey with the BatImager, processing the whole sky significance map and estimating rates and significances in the locations of the Roma-BZCAT blazars. We considered a source detected if its significance was above 4.8 σ in at least one of the considered energy bands (15–150 keV, 15–30 keV, 15–70 keV). We found a significant hard X-ray counterpart for 54 Roma-BZCAT sources:

- 14 BL Lac objects;

- 32 FSRQ;

- 8 unclassified blazars.

In Fig. 1 we show the location of the detected sources in Palermo BAT survey mosaic image of the whole sky. Comparing these detections with the ones we obtained from a list of ∼2600 random positions on the sky, we estimate that there is a 10% chance that one of our sources is due to spurious association. The source properties (name, position, count rates and significance of detection in the 15–150 keV, 15–30 keV and 15–70 keV energy bands) are reported in Table 1.
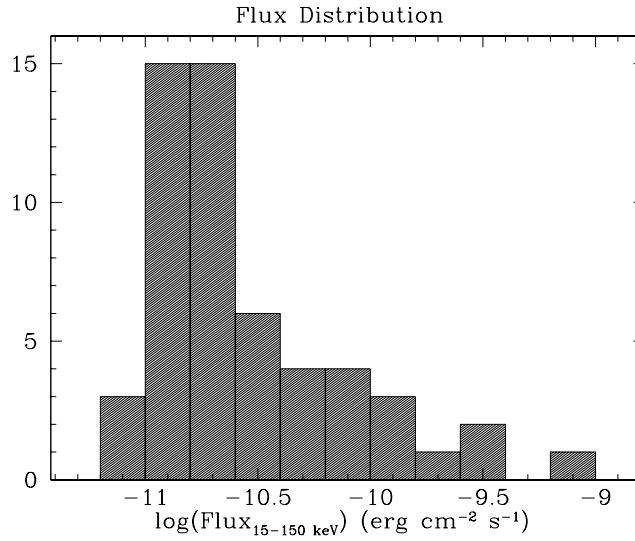
Flux Distribution

Figure 2: Flux distribution for Roma-BZCAT blazars detected in the BAT survey.

The flux distribution of the detected sources is reported in Fig. 2. We detect sources in the $10^{-11} - 10^{-9}$ ergs cm^{-2} s^{-1} range.

In Fig. 3 we show the hardness ratios (30–70/15–30 keV vs. 150–70/15–30 keV). The distribution of BL Lac objects and FSRQ have no significant differences in this plane.
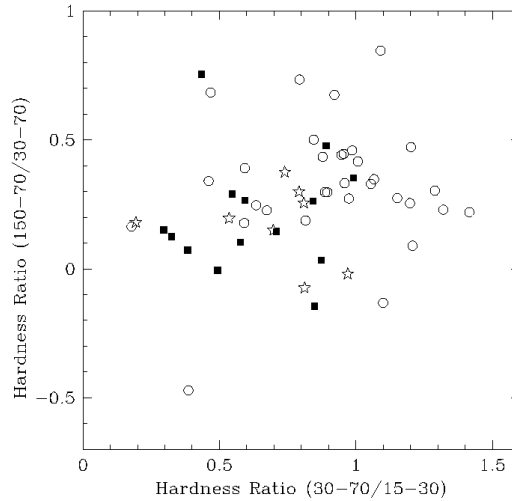

Figure 3: Hardness ratios for for Roma-BZCAT blazars detected in the BAT survey. Filled squares indicate FSRQ, open circles indicate BL Lac objects and stars indicate unclassified sources.

Searching in the literature, we were able to find a determination of the redshift for 53 sources. We show the redshift distribution in Fig. 4. As expected, most of the sources are at relatively low redshift, but we detect blazars up to z∼3.5. The inferred luminosity distribution is shown in Fig. 5. We observe luminosities in the $10^{42} - 10^{48}$ ergs s^{-1} range, with more than 50% of the objects above 10^{46} ergs s^{-1}.

In order to better constrain the properties of these objects, we plan to make use of data in other

bands of the electromagnetic spectrum, already existing in the literature or in the archives, or to be obtained in future observations. In particular, we will check for differences in the observed properties of the various blazar subclasses (HBL, LBL, IBL, FSRQ) in the BAT energy band and if and how these properties correlate with observations in other bands of the electromagnetic spectrum.
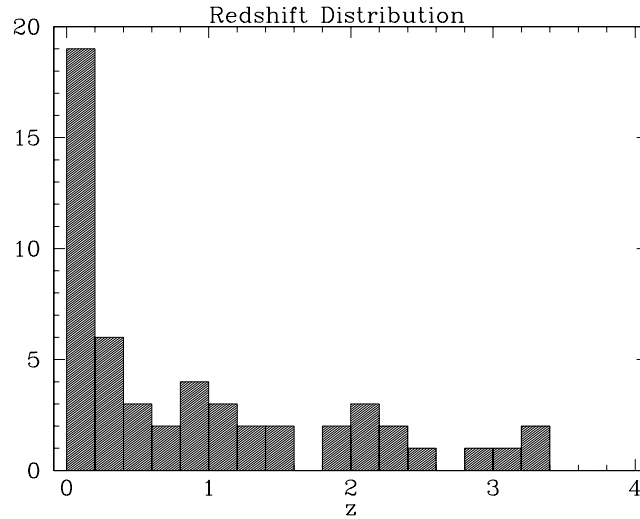
Figure 4: Redshift distribution for Roma-BZCAT blazars detected in the BAT survey.
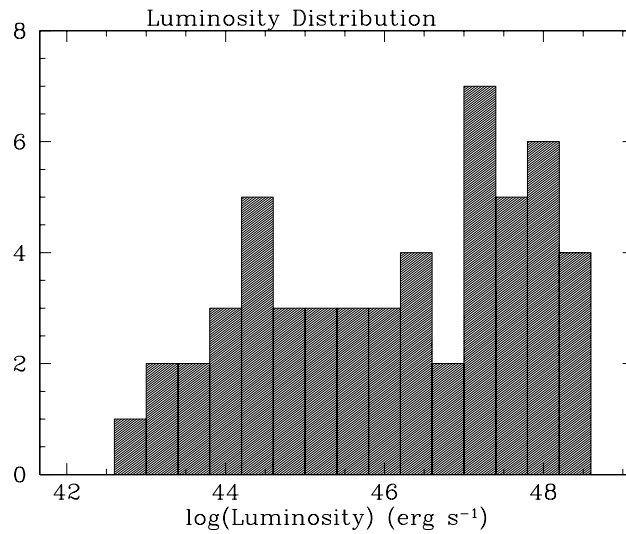
Figure 5: Luminosity distribution for Roma-BZCAT blazars detected in the BAT survey.

4

Table 1: Roma-BZCAT blazars detected in the BAT survey.

ID	Name	Alt. name	RA	Dec	15–150 keV band		15–30 keV band		15–70 keV band	
					Rate	σ	Rate	σ	Rate	σ
			(deg)	(deg)	$(10^{-5}$ cts s$^{-1})$		$(10^{-5}$ cts s$^{-1})$		$(10^{-5}$ cts s$^{-1})$	
1	BZQJ0010+1058	MRK 1501	2.629	10.97	(3.5 ± 0.4)	9.8	(1.9 ± 0.2)	8.6	(3.2 ± 0.3)	10.0
2	BZQJ0017+8135	[HB89] 0014+813	4.285	81.59	(2.0 ± 0.3)	6.4	(1.1 ± 0.2)	5.0	(1.6 ± 0.3)	5.6
3	BZBJ0035+5950	1ES 0033+595	8.969	59.83	(3.1 ± 0.4)	8.6	(2.3 ± 0.2)	9.5	(3.0 ± 0.3)	8.8
4	BZUJ0048+3157	NGC 0262	12.196	31.96	(15.7 ± 0.3)	50.9	(7.8 ± 0.2)	38.5	(14.1 ± 0.3)	51.6
5	BZBJ0123+3420	RGB J0123+343	20.785	34.35	(1.7 ± 0.3)	5.3	(1.0 ± 0.2)	5.0	(1.6 ± 0.3)	5.6
6	BZQJ0217+7349	1ES 0212+735	34.378	73.83	(3.7 ± 0.3)	10.7	(1.6 ± 0.2)	7.0	(3.2 ± 0.3)	10.1
7	BZBJ0232+2017	1ES 0229+200	38.202	20.29	(2.5 ± 0.4)	6.6	(1.5 ± 0.3)	5.5	(2.7 ± 0.3)	8.0
8	BZBJ0235-2938	RX J023536.8-293842	38.903	-29.65	(2.1 ± 0.3)	7.0	(0.9 ± 0.2)	4.7	(1.7 ± 0.3)	6.5
9	BZUJ0319+4130	1ES 0316+413	49.950	41.51	(10.9 ± 0.4)	27.9	(8.9 ± 0.2)	36.6	(10.6 ± 0.3)	30.7
10	BZQJ0336+3218	RX J0336.5+3218	54.125	32.31	(3.3 ± 0.4)	7.8	(1.5 ± 0.3)	5.8	(2.9 ± 0.4)	7.8
11	BZBJ0349-1159	RBS 0476	57.347	-11.99	(2.3 ± 0.3)	7.3	(1.3 ± 0.2)	6.1	(1.9 ± 0.3)	6.5
12	BZQJ0405-1308	PKS 0403-13	61.392	-13.14	(1.6 ± 0.3)	4.9	(0.7 ± 0.2)	3.1	(1.6 ± 0.3)	5.4
13	BZUJ0433+0521	3C 120	68.296	5.35	(10.9 ± 0.4)	26.3	(5.2 ± 0.3)	18.7	(9.1 ± 0.4)	25.4
14	BZUJ0522-3627	ESO 362-G021	80.741	-36.46	(3.1 ± 0.3)	10.7	(1.9 ± 0.2)	9.9	(2.9 ± 0.3)	11.1
15	BZQJ0525-4557	PKS 0524-460	81.381	-45.96	(2.0 ± 0.3)	7.4	(0.8 ± 0.2)	4.3	(1.5 ± 0.3)	6.1
16	BZQJ0539-2839	[HB89] 0537-286	84.976	-28.67	(2.7 ± 0.3)	9.0	(1.1 ± 0.2)	5.4	(2.2 ± 0.3)	8.0
17	BZBJ0550-3216	[HB89] 0548-322	87.669	-32.27	(3.4 ± 0.3)	11.2	(2.0 ± 0.2)	9.4	(3.1 ± 0.3)	11.7
18	BZBJ0613+7107	87GB 060751.7+710809	93.430	71.12	(3.3 ± 0.3)	10.8	(1.4 ± 0.2)	6.3	(2.8 ± 0.3)	9.8
19	BZQJ0632-5404	SGRS J0631-5405	98.007	-54.08	(1.4 ± 0.3)	4.2	(1.1 ± 0.2)	5.1	(1.6 ± 0.3)	5.2
20	BZQJ0746+2549	B2 0743+25	116.608	25.82	(3.9 ± 0.4)	10.6	(1.4 ± 0.2)	5.8	(3.1 ± 0.3)	9.4
21	BZQJ0747-6744	PMN J0746-6744	116.771	-67.74	(23.2 ± 0.3)	70.3	(13.7 ± 0.2)	60.0	(21.7 ± 0.3)	69.3
22	BZQJ0841+7053	[HB89] 0836+710	130.351	70.89	(6.8 ± 0.3)	23.1	(2.8 ± 0.2)	13.7	(5.8 ± 0.3)	21.3
23	BZQJ1044+8054	[HB89] 1039+811	161.096	80.91	(1.8 ± 0.3)	6.0	(0.7 ± 0.2)	3.6	(1.6 ± 0.3)	5.9
24	BZBJ1103-2329	2MASX J11033765-2329307	165.906	-23.49	(1.8 ± 0.4)	5.2	(1.4 ± 0.2)	5.8	(1.8 ± 0.3)	5.5
25	BZBJ1104+3812	MRK 0421	166.114	38.21	(17.5 ± 0.3)	62.8	(12.4 ± 0.2)	67.4	(17.1 ± 0.3)	68.1
26	BZQJ1107+7232	[HB89] 1104+728	166.924	72.54	(11.1 ± 0.3)	40.4	(5.6 ± 0.2)	30.8	(10.2 ± 0.2)	42.3

ID	Name	Alt. name	RA	Dec	15–150 keV band		15–150 keV band		15–150 keV band	
					Rate	σ	Rate	σ	Rate	σ
27	BZQJ1130-1449	[HB89] 1127-14	172.529	-14.82	(4.2 ± 0.4)	11.6	(1.9 ± 0.2)	7.6	(3.5 ± 0.3)	11.0
28	BZQJ1153+4931	SBS 1150+497	178.352	49.52	(1.5 ± 0.3)	5.5	(0.6 ± 0.2)	3.5	(1.3 ± 0.2)	5.4
29	BZBJ1210+3929	[HB89] 1207+397	182.611	39.49	(44.4 ± 0.3)	143.7	(21.5 ± 0.2)	111.4	(39.6 ± 0.3)	154.6
30	BZQJ1222+0413	[HB89] 1219+044	185.594	4.22	(2.4 ± 0.4)	6.9	(0.9 ± 0.2)	4.0	(2.1 ± 0.3)	6.9
31	BZQJ1224+2122	PG 1222+216	186.227	21.38	(1.4 ± 0.3)	5.1	(0.7 ± 0.2)	3.8	(1.5 ± 0.3)	5.9
32	BZQJ1229+0203	3C 273	187.278	2.05	(40.8 ± 0.4)	104.5	(18.9 ± 0.2)	75.6	(35.8 ± 0.3)	108.2
33	BZQJ1256-0547	3C 279	194.046	-5.79	(4.1 ± 0.4)	10.4	(2.2 ± 0.3)	8.1	(3.5 ± 0.4)	10.0
34	BZUJ1325-4301	Centaurus A	201.365	-43.02	(115.6 ± 0.5)	219.8	(57.0 ± 0.4)	159.0	(102.1 ± 0.5)	199.3
35	BZQJ1332-0509	PKS 1329-049	203.018	-5.16	(1.9 ± 0.4)	5.2	(0.7 ± 0.3)	2.6	(1.6 ± 0.3)	5.1
36	BZUJ1413-0312	NGC 5506	213.312	-3.21	(26.9 ± 0.4)	65.4	(14.9 ± 0.3)	52.3	(25.3 ± 0.4)	68.6
37	BZBJ1428+4240	RBS 1399	217.136	42.67	(2.5 ± 0.3)	9.3	(1.4 ± 0.2)	7.3	(2.4 ± 0.2)	9.9
38	BZQJ1504+1029	[HB89] 1502+106	226.104	10.49	(2.6 ± 0.4)	6.6	(1.6 ± 0.3)	5.4	(2.3 ± 0.4)	6.5
39	BZQJ1512-0905	PKS 1510-08	228.210	-9.10	(5.0 ± 0.5)	10.7	(2.2 ± 0.4)	6.2	(4.1 ± 0.4)	9.4
40	BZBJ1653+3945	MRK 0501	253.467	39.76	(5.8 ± 0.4)	14.2	(3.4 ± 0.3)	13.2	(5.3 ± 0.4)	14.3
41	BZUJ1719+4858	RX J1719.2+4858	259.810	48.98	(2.5 ± 0.3)	7.8	(1.4 ± 0.2)	6.7	(2.6 ± 0.3)	8.7
42	BZQJ1826-3650	NVSS J182608-365049	276.534	-36.85	(9.5 ± 0.6)	16.5	(7.9 ± 0.5)	16.8	(9.3 ± 0.5)	17.3
43	BZUJ1829+4844	3C 380	277.382	48.75	(1.9 ± 0.4)	5.5	(1.0 ± 0.2)	4.3	(2.0 ± 0.3)	6.1
44	BZQJ1833-2103	PKS 1830-21	278.416	-21.06	(8.5 ± 0.7)	11.4	(3.5 ± 0.5)	6.8	(7.2 ± 0.7)	10.4
45	BZBJ1959+6508	2MASX J19595975+6508547	299.999	65.15	(4.5 ± 0.3)	13.5	(3.0 ± 0.2)	14.1	(4.5 ± 0.3)	14.7
46	BZQJ2129-1538	[HB89] 2126-158	322.300	-15.64	(2.4 ± 0.4)	5.6	(1.1 ± 0.3)	3.8	(2.1 ± 0.4)	5.6
47	BZQJ2148+0657	[HB89] 2145+067	327.022	6.96	(2.2 ± 0.4)	5.6	(0.8 ± 0.3)	3.2	(1.9 ± 0.4)	5.5
48	BZQJ2151-3027	[HB89] 2149-307	327.981	-30.46	(7.4 ± 0.4)	19.6	(3.1 ± 0.3)	11.5	(6.1 ± 0.3)	17.9
49	BZBJ2202+4216	BL Lac	330.680	42.28	(2.8 ± 0.4)	7.4	(1.5 ± 0.2)	6.5	(2.8 ± 0.3)	8.3
50	BZQJ2219+2613	2MASX J22194971+26132	334.957	26.22	(1.8 ± 0.4)	5.2	(1.0 ± 0.2)	4.4	(1.7 ± 0.3)	5.6
51	BZQJ2229-0832	[HB89] 2227-088	337.417	-8.55	(2.0 ± 0.4)	5.0	(0.8 ± 0.3)	3.3	(1.5 ± 0.4)	4.2
52	BZQJ2232+1143	[HB89] 2230+114	338.152	11.73	(2.8 ± 0.4)	7.8	(1.2 ± 0.2)	4.7	(2.3 ± 0.3)	6.9
53	BZQJ2253+1608	3C 454.3	343.490	16.15	(11.8 ± 0.4)	32.3	(4.8 ± 0.2)	20.1	(9.6 ± 0.3)	29.0
54	BZQJ2327+0940	PKS 2325+093	351.890	9.67	(2.3 ± 0.4)	6.0	(0.8 ± 0.3)	3.0	(1.6 ± 0.4)	4.5

Acknowledgments

References

[1] Barthelmy, S. D., et al., 2005, SSRv, 120, 143

[2] Gehrels, N., et al., 2004, ApJ, 611, 1005

[3] Massaro, E.et al., 2008, MmSAI, 79, 262

[4] Segreto, A., et al., 2008, in preparation